The composite development and structure of intense synoptic-scale Arctic cyclones

Alexander F. Vessey[1,2], Kevin I. Hodges[2,3], Len C. Shaffrey[2,3], and Jonathan J. Day[3]

[1]AXA XL, 20 Gracechurch Street, London, UK, EC3V 0BG
[2]Department of Meteorology, University of Reading, Earley Gate, Reading RG6 6BB, UK
[3]National Centre for Atmospheric Science, University of Reading, Earley Gate, Reading RG6 6BB, UK
[4]ECMWF, Shinfeld Park, Reading RG2 9AX, UK

Correspondence: Alexander F. Vessey (alexander.vessey@axaxl.com)

Abstract.

Understanding the location and intensity of hazardous weather across the Arctic is important for assessing risks to infrastructure, shipping, and coastal communities. Key hazards driving these risks are extreme near-surface winds, high ocean waves and heavy precipitation, which are dependent on the structure and development of intense synoptic-scale cyclones.

5   This study aims to describe the typical lifetime, structure, and development of a large sample of past intense winter (DJF) and summer (JJA) synoptic-scale Arctic cyclones, using a storm compositing methodology applied to the ERA5 reanalysis.

Results show that the composite development and structure of intense Arctic summer cyclones is different to that of intense winter Arctic and North Atlantic Ocean extra-tropical cyclones, and to that described in conceptual models of extra-tropical and Arctic cyclones. The composite structure of intense Arctic summer cyclones shows that they typically undergo a

10   structural transition around the time of maximum intensity from having a baroclinic structure to an axi-symmetric cold-core structure throughout the troposphere, with a low-lying tropopause and large positive temperature anomaly in the lower stratosphere. Arctic summer cyclones are also found to have longer lifetimes than these other cyclones, potentially causing prolonged hazardous and disruptive weather conditions in the Arctic.

1   Introduction

15   Recent reductions in Arctic sea ice extent (Stroeve et al., 2012; National Snow & Ice Data Center, 2020; Simmonds and Li, 2021) have opened up shorter shipping routes between ports in North America, Europe, and Asia (Melia et al., 2016), access to previously inaccessible natural resources such as oil (Harsem et al., 2015), and new destinations for tourism (Maher, 2017). Consequently, the number of ships navigating the Arctic with people and valuable goods onboard has increased in recent years (Babin et al., 2020; Li et al., 2021). Given that Arctic sea ice extent will continue to reduce over the 21st century in response

20   to further global warming (Stroeve et al., 2012; Notz and SIMIP Community, 2020; Årthun et al., 2021), human activity in the Arctic is expected to increase further as the Arctic Ocean becomes increasingly accessible. But as the Arctic becomes increasingly used for shipping, oil exploration and tourism, the exposure to hazardous weather associated with Arctic cyclones, may increase.

The structure of extra-tropical cyclones has been a focal point of scientific research for over 100 years, as they can have a damaging impact on populous areas such as Europe (Browning, 2004; Leckebusch et al., 2007; Pinto et al., 2012). Bjerknes (1919, 1922) were among the first to describe the typical structure and locality of hazardous weather within extra-tropical cyclones, and proposed the Norwegian Cyclone Model - a conceptual model of extra-tropical cyclone development and structure. It is now understood that the locality of hazardous weather within an extra-tropical cyclone is dependent on its structure, with high precipitation typically occurring at the location of weather fronts (Bjerknes, 1919; Dacre, 2020), and high low-level wind speeds occurring at the locations of low-level conveyor belts and features such as sting jets (Browning, 1997, 2004; Martínez-Alvarado et al., 2014; Schultz and Browning, 2017).

In addition to the Norwegian Cyclone Model, the Shapiro-Keyser Model describes an alternative structural development cycle of extra-tropical cyclones (Shapiro and Keyser, 1990). The initial stages of each model are similar, but the Shapiro-Keyser Model describes how extra-tropical cyclones may undergo frontal fracture during their mature phase and develop a warm core (Shapiro and Keyser, 1990). Alternatively, the Norwegian Cyclone Model describes how extra-tropical cyclones may continue to undergo occlusion during their mature phase, where the cold air mass wraps around the cyclone centre into the warm air mass (Bjerknes, 1919, 1922). Case studies of past extra-tropical cyclones have been identified that appear to follow a similar structural development cycle described in each model (e.g., Carlson, 1980; Browning, 2004), and it is generally agreed that a particular extra-tropical cyclone may follow either models, or even a combination of both (Schultz et al., 1998).

It is currently unclear whether Arctic cyclones have a similar structural development cycle to extra-tropical cyclones. The analysis of some individual Arctic summer cyclones suggests that they may have a different structure to extra-tropical cyclones (Tanaka et al., 2012; Aizawa et al., 2014; Aizawa and Tanaka, 2016; Tao et al., 2017). Aizawa and Tanaka (2016) showed that 'The Great Arctic Cyclone of 2012' developed an axi-symmetric cold core and barotropic structure during its mature phase, which contrasts with the Norwegian Cyclone Model (Bjerknes, 1919, 1922) and the Shapiro-Keyser Model (Shapiro and Keyser, 1990). This unique structure is also identified in five other past Arctic cyclones that occurred in August 2006, August 2007, and June 2008 (Tanaka et al., 2012), June 2008 (Aizawa et al., 2014; Aizawa and Tanaka, 2016) and September 2010 (Tao et al., 2017). Tanaka et al. (2012) and Tao et al. (2017) showed that in their Arctic cyclone case studies, a lower stratospheric positive potential vorticity anomaly (i.e., Tropopause Polar Vortices - TPVs) played a decisive role in each cyclone's development. Simmonds and Rudeva (2014) also showed that TPVs influenced the development of 54 out of 60 intense Arctic cyclones, with the sample size of 60 being comprised of the five most intense Arctic cyclones per calendar month from 1979-2009. However, a more systematic study that examines a greater sample of Arctic cyclones is required to show this unique cyclone structure in generality.

Some Arctic cyclones have also been found to have exceptionally long lifetimes, potentially causing prolonged hazardous weather conditions in the Arctic (Simmonds and Rudeva, 2012, 2014; Aizawa and Tanaka, 2016; Tao et al., 2017). Cyclones are associated with rough sea conditions including extreme near-surface wind speeds and high ocean waves (Thomson and Rogers, 2014; Liu et al., 2016; Waseda et al., 2018; Squire, 2020; Waseda et al., 2021). Arctic cyclones can also break-up sea ice, which may then become mobile and drift toward shipping lanes, creating an additional hazard (Simmonds and Keay, 2009; Asplin et al., 2012; Parkinson and Comiso, 2013; Peng et al., 2021). Simmonds and Rudeva (2012) showed that 'The Great

Arctic Cyclone of 2012' had a lifetime greater than 10 days. Moreover, the June 2008 case study from Aizawa and Tanaka (2016) had a lifetime greater than 14 days. It is currently uncertain how typical these longer-lived Arctic cyclones are.

Previous research on the structure and development of Arctic cyclones has primarily focused on case studies occurring in summer (Tanaka et al., 2012; Aizawa et al., 2014; Aizawa and Tanaka, 2016; Tao et al., 2017). But the spatial distribution of Arctic cyclones has been found to vary seasonally (Reed and Kunkel, 1960; Serreze et al., 2001; Simmonds et al., 2008; Crawford and Serreze, 2016; Vessey et al., 2020). In winter, Arctic cyclone track density is typically highest over the Greenland, Norwegian and Barents Seas and over the Canadian Archipelago, whereas in summer, Arctic cyclone track density is typically highest over the coastline of Eurasia and the Arctic Ocean (Vessey et al., 2020). The impact of the environmental conditions on the development of Arctic cyclones during winter and summer is an open question.

This study aims to describe the typical lifetime, structure, and development of a large sample of past intense synoptic-scale winter (DJF) and summer (JJA) Arctic cyclones, using a storm compositing methodology. The focus is on intense cyclones that would most endanger human activity. Winter extra-tropical cyclones occurring over the North Atlantic Ocean are used as a reference to compare with intense winter and summer Arctic cyclones, as they have been investigated more extensively in previous research (e.g., Bjerknes, 1919, 1922; Shapiro and Keyser, 1990; Browning, 1997, 2004; Catto et al., 2010; Varino et al., 2019; Wickström et al., 2020). Conceptual models of extra-tropical cyclone structure and development are also primarily based on the analysis of winter extra-tropical cyclones. Therefore, comparing Arctic cyclones with winter North Atlantic Ocean cyclones allows for a more direct comparison to these conceptual models. The aim of this study will be achieved by answering the following questions:

- What are the typical lifetimes of intense winter (DJF) and summer (JJA) Arctic cyclones?

- How does the composite structure of intense winter and summer Arctic cyclones develop before and after the time of maximum intensity?

- How does the lifetime and composite structure of intense winter and summer Arctic cyclones differ to that of intense winter North Atlantic Ocean extra-tropical cyclones?

This paper continues in Section 2, where the methods used in this study are described. This includes a description of the data, storm tracking method and storm compositing method used. Results are then described in Section 3, detailing the typical lifetimes, spatial distribution and composite structure of intense synoptic-scale winter and summer Arctic cyclones and winter North Atlantic Ocean extra-tropical cyclones. Finally, a summary of the main conclusions is given in Section 4.

2 Methodology

2.1 Data

This study uses data from the European Centre for Medium-Range Weather Forecasts (ECWMF) fifth generation atmospheric reanalysis (ERA5) (Hersbach et al., 2020). Reanalysis datasets provide spatially and temporally homogeneous datasets, which

combine past observations of the atmosphere with current atmospheric models to produce the best approximation of past atmospheric states. ERA5 is the latest and highest resolution reanalyses to be produced by the ECMWF.

ERA5 includes global atmosphere data from 1979 - present. Data is output at a horizontal resolution of approximately 31 km (or TL639), with 137 levels up to 0.01 hPa. Historical observations are quality controlled and assimilated into the ECMWF IFS (41r2) model using a four-dimensional variational data assimilation (4D-Var) scheme to create a best approximation of the past atmosphere. From ERA5, the surface mean sea level pressure (MSLP) field, and the temperature, wind (u-component and v-component), vertical velocity, relative humidity, and potential vorticity fields over nine pressure levels (925 hPa, 850 hPa, 700 hPa, 600 hPa, 500 hPa, 400 hPa, 300 hPa, 200 hPa and 100 hPa) are used at 6-hour time intervals (00:00, 06:00, 12:00 and 18:00 UTC).

2.1.1 Storm tracking

Cyclones are identified in ERA5 using the storm tracking algorithm developed by Hodges (1994, 1995, 1999). Vessey et al. (2020) showed that when using this storm tracking algorithm and identical filtering criteria, tracking cyclones based on 850 hPa relative vorticity generally identifies more Arctic cyclones than those based on MSLP. Therefore, Arctic cyclones in this study are identified as maxima in the 850 hPa relative vorticity field. This field is first spectrally truncated to a spectral resolution of T42 and is filtered to remove the planetary scales for total wavenumbers less than or equal to 5. This ensures that synoptic-scale systems that are independent of large-scale forcings are focused upon.

Cyclone features are then identified as maxima in the 850 hPa relative vorticity field at each timestep. Features within the maximum displacement factor (5° for the regions north of 30°N) are then grouped into cyclone tracks using a nearest-neighbour approach, which links feature points in consecutive timesteps (Hodges, 1999). Once all cyclone tracks have been identified in ERA5 from 1979 - 2020, they are then filtered to retain cyclones that last more than 2 days and travel more than 1000 km. This further ensures that synoptic-scale and mobile cyclones are focused upon. Arctic cyclones are defined in this study as any cyclone that travels north of 65°N. For comparison, Arctic cyclones are contrasted with extra-tropical winter cyclones that occurred over the North Atlantic Ocean, between -53 to 20°E and 30 - 65°N.

2.2 Storm compositing

The composite (averaged) structure of cyclones is examined using a system-centred composite method, which is described in Bengtsson et al. (2007, 2009) and Catto et al. (2010). A composite method can identify the general structure of a group of cyclones, by taking an average of atmospheric fields across a space centred on each cyclone's centre. A composite is the average structure of multiple cyclones. It allows for the identification of the general structure of a group of cyclones, but without smaller scale features that tend to be smoothed out by the method. The composite method has three steps: storm selection, storm rotation and lifetime positioning.

Firstly, the 100 most intense winter North Atlantic Ocean extra-tropical cyclones and Arctic winter and summer cyclones with the lowest full resolution MSLP minima between 1979 and 2020 in ERA5 are identified (storm selection). Figure S1 in the supplementary material shows the difference in timestep between the point of maximum T42 filtered 850 hPa relative

vorticity and point of full resolution minimum MSLP of each cyclone that contributes to each cyclone composite. For each class of cyclone, the point of maximum intensity per atmospheric variable in each cyclone's lifecycle generally coincide, and the difference in timestep is shown to be mostly -1, 0, or 1. Therefore the choice here to filter to the 100 most intense cyclones by minimum full resolution MSLP rather than maximum T42 filtered 850 hPa relative vorticity does not significantly change the composites computed, as the lifetime positioning timestep of each cyclone generally coincide.

To be characterised as an Arctic cyclone, cyclones must have 60% of their track points in the Arctic (north of 65°N) and their maximum intensity (i.e., minimum MSLP) in the Arctic. This is to ensure that intense Arctic cyclones that spend most of their lifetime in the Arctic are selected. A similar procedure was followed to identify the 100 most intense cyclones that occurred over the North Atlantic Ocean region (between -53 to 20°E and 30 - 65°N) from 1979 - 2020.

The atmospheric fields associated with each cyclone are then sampled onto a 20° longitude-latitude rectangular grid with a horizontal resolution of 0.5°, so that the origin 0,0 is centred on the cyclone centre (the point of minimum MSLP). This grid is initially setup to be centred on the equator and ensures a fair spatial comparison between cyclones that occur at different latitudes. This grid can then be rotated so that each cyclone is orientated according to the it's propagation direction, or the geographical orientation of each cyclone is kept before an average is made over all cyclones (storm rotation). The cyclone's propagation direction is determined using a pair of consecutive track points for the points before, at and after each track point, and then these vectors are averaged to smooth the direction (Catto et al., 2010).

Both approaches of storm rotation have been used in previous research (e.g., Wang and Rogers, 2001; Bauer and Del Genio, 2006; Bengtsson et al., 2007, 2009; Catto et al., 2010). An advantage of rotating each cyclone to its propagation direction before averaging is that system-relative winds can be determined, which are independent of the cyclone's propagation velocity. This can help to determine features such as conveyor belts within the cyclone composite (Catto et al., 2010). The occurrence of these conveyor belts has also been shown to coincide with the occurrence of extreme weather e.g., high wind speeds (Browning, 2004; Martínez-Alvarado et al., 2014) and high precipitation (Catto et al., 2015). Thus, a further advantage of rotating each cyclone relative to its propagation direction before averaging, is that it may uncover details of the occurrence of these conveyor belts and extreme weather within each class of cyclone. In this study, cyclone composites are produced by rotating each cyclone to a common direction of propagation before averaging, so that it can be determined whether conveyor belts, which have been shown to occur in typical extra-tropical cyclones (e.g., Browning, 1997), also occur in Arctic cyclones.

Composites are produced by taking an average of the atmospheric fields around the cyclone centre at various points in each cyclone's lifecycle (lifetime positioning). Composites in this study are produced at the time of maximum intensity, when each cyclone reaches their MSLP minima. This is to determine the structure of cyclones when they are at their most hazardous. The development of each composite is also determined at timesteps up to 48 hours before and up to 192 hours after the time of maximum intensity at 48-hour intervals. Only cyclones that survive up 192 hours after the time of maximum intensity contribute to the cyclone composite at these lifetime positions. Each cyclone is orientated according to its propagation direction at that lifetime position point before averaging and computing the composite over all cyclones. Temperature anomalies are calculated by subtracting the temperature value at each spatial point from the mean temperature across the horizontal 20° longitude-latitude domain at each vertical level.

3 Results

3.1 Cyclone Lifetime

160 The 100 most intense winter and summer Arctic cyclones are typically less intense than the 100 most intense North Atlantic Ocean winter extra-tropical cyclones (see Figure 1a). The mean minimum MSLP of the 100 most intense North Atlantic Ocean winter extra-tropical cyclones is 945.5 hPa, but is 953.8 hPa and 974.6 hPa for the 100 most intense Arctic winter and summer cyclones respectively. The mean lifetime of the 100 most intense Arctic summer cyclones is however much greater than that of winter Arctic cyclones and North Atlantic Ocean extra-tropical cyclones (see Figure 1). This is in agreement with Simmonds

165 and Rudeva (2014), who show that the most intense Arctic cyclones are typically more intense in winter than in summer but have a longer lifetime in summer than in winter.

The mean lifetime of the 100 most intense Arctic summer cyclones (9.7 days) is more than 3 days greater than that of the 100 most intense Arctic winter cyclones (6.1 days) and more than 4 days greater than that of the 100 most intense North Atlantic Ocean winter extra-tropical cyclones (5.4 days) (see Figure 1a). This is also shown by more of the 100 most intense Arctic

170 summer cyclones existing longer before and after their time of maximum intensity (see Figure 1a). The modal lifetime of the 100 most intense Arctic summer cyclones is also greater than 10 days, with just under half of these cyclones (44) surpassing this threshold (see Figure 1b). This is much greater than the modal lifetime of the 100 most intense winter Arctic and North Atlantic Ocean extra-tropical cyclones (4-6 days). With a longer lifetime, Arctic summer cyclones may cause prolonged hazardous weather conditions in the Arctic, such as extreme near-surface winds and high ocean waves (Thomson and Rogers, 2014; Liu

175 et al., 2016; Waseda et al., 2018; Squire, 2020; Waseda et al., 2021).

3.2 Arctic cyclone spatial distribution

The track density of Arctic cyclones has been found in previous research to vary seasonally (Reed and Kunkel, 1960; Serreze et al., 2001; Simmonds et al., 2008; Crawford and Serreze, 2016; Vessey et al., 2020). Arctic cyclone track density is typically highest in winter over the Greenland, Norwegian and Barents Seas, and over the Canadian Archipelago, whereas in summer,

180 Arctic cyclone track density is typically highest over the coastline of Eurasia and the Arctic Ocean (Simmonds et al., 2008; Vessey et al., 2020). This is reflected in the spatial distribution of the locations of maximum intensity of the 100 most intense Arctic winter and summer cyclones (see Figure 2). Generally, the 100 most intense winter Arctic cyclones have their maximum intensity over the Greenland, Norwegian and Barents Seas (see Figure 2). In contrast, the 100 most intense Arctic summer cyclones tend to have their maximum intensity over higher latitudes and over the Arctic Ocean that is north of the Eurasian

185 coastline and the Bering Strait (see Figure 2). This was similarly shown in Simmonds and Rudeva (2014).

Over the past few decades, the Arctic has experienced the greatest change in mean surface temperature than any other region on Earth (Lenssen et al., 2019; GISTEMP Team, 2021). This raises the question, has the occurrence of intense Arctic cyclones changed over the last few decades? Figure S2 in the supplementary material shows a timeseries by year of the occurrence of each cyclone within the sample of the 100 most intense per cyclones class. Overall, there is no visible trend in the frequency

190 of intense winter North Atlantic cyclones (see Figure S2a in supplementary material), winter Arctic cyclones (Figure S2b in
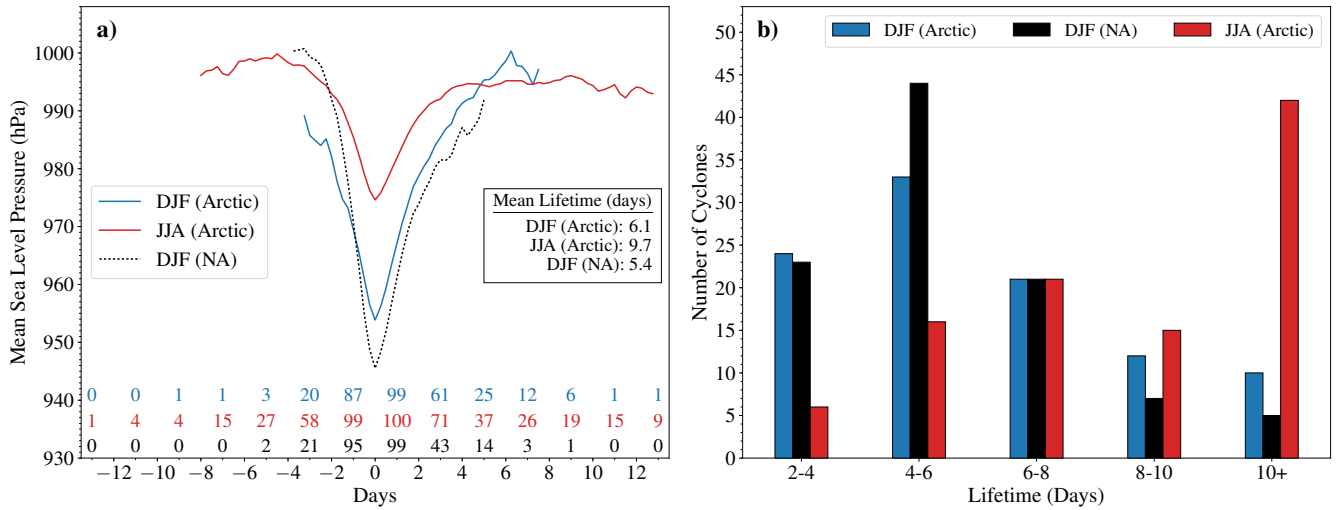
Figure 1. Lifecycles of the 100 most intense winter (DJF) and summer (JJA) Arctic cyclones and winter North Atlantic (NA) Ocean extra-tropical cyclones between 1979 and 2020. **a)** The mean composite lifecycle development in intensity (MSLP), when cyclones are centred at the time of their maximum intensity (minimum MSLP) and where at least 10 cyclones exist at each time interval. The numbers indicate how many cyclones exist at each time interval. **b)** The distribution in the lifetimes of the 100 most intense winter and summer Arctic cyclones and winter North Atlantic (NA) Ocean extra-tropical cyclones.

supplementary material), or summer Arctic cyclones (Figure S2c in supplementary material), when considering the occurrence of the 100 most intense cyclones per class.

3.3 Horizontal composite structure at the time of maximum intensity

The 100 most intense summer Arctic cyclones are less intense than winter Arctic and North Atlantic Ocean extra-tropical cyclones (see Figure 1). Thus, the minimum MSLP of the Arctic summer cyclone composite at the time of maximum intensity (976.6 hPa) is higher than the winter Arctic cyclone (958.8 hPa) and North Atlantic Ocean extra-tropical cyclone (949.2 hPa) composites (see Figure 3a, 3d, and 3g). The pressure gradients are tighter in the Arctic winter cyclone composite than in the Arctic summer cyclone composite, but tightest in the North Atlantic Ocean winter extra-tropical cyclone composite.

The Arctic summer cyclone composite also appears to be smaller in size than the Arctic winter and North Atlantic Ocean cyclone composites. This is inferred by the last closed isobar not exceeding the 2200 x 2200 km domain in the Arctic summer cyclone composite (see Figure 3g). In contrast, the last closed isobar exceeds of the winter Arctic and North Atlantic Ocean cyclone composite the 2200 x 2200 km domain (see Figure 3a and 3d). Moreover, the Arctic summer cyclone composite is more axi-symmetric than the winter Arctic and North Atlantic Ocean extra-tropical cyclone composites (see Figure 3a, 3d, and 3g), which have tighter pressure gradients below the composite cyclone centre than above the composite cyclone centre.
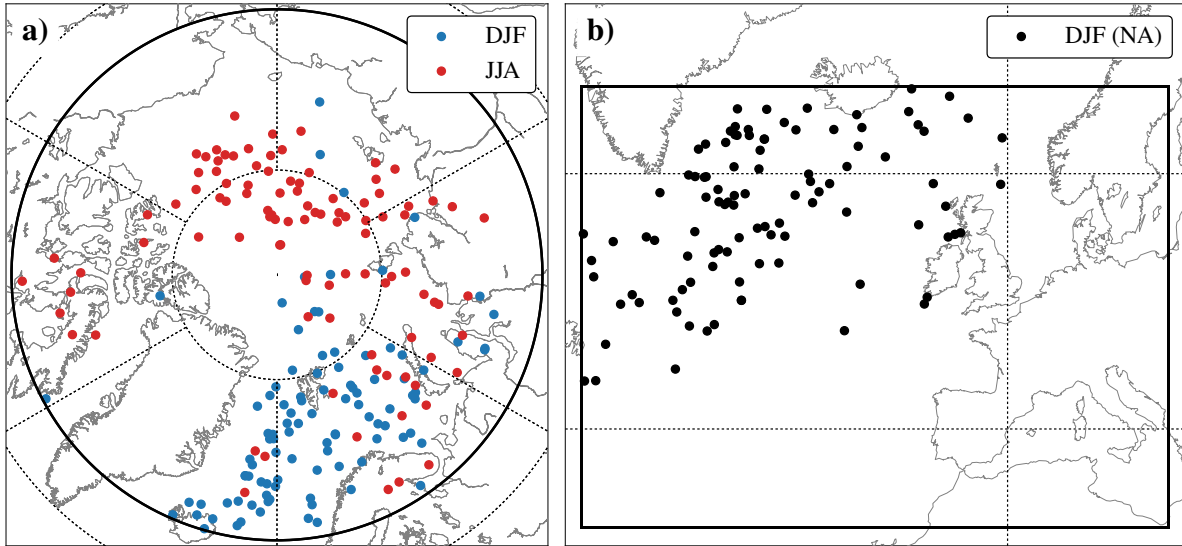
Figure 2. The locations of the points of maximum intensity (minimum MSLP) of each of the 100 most intense **a)** winter (DJF) and summer (JJA) Arctic cyclones and **b)** winter North Atlantic (NA) Ocean extra-tropical cyclones between 1979 and 2020. Longitudes are shown every $60°$E, and latitudes are shown at **a)** $80°$N, $65°$N (bold) and $50°$N, and **b)** $60°$N and $40°$N, with the thick black lines indicating the domains used for selecting each class of cyclone.

205  The maximum 850 hPa earth-relative wind speeds are weaker in the Arctic summer cyclone composite (20.9 m s^{-1}) than the Arctic winter cyclone composite (24.5 m s^{-1}) and the North Atlantic Ocean winter extra-tropical cyclone composite (32.3 m s^{-1}) (see Figure 3b, 3e and 3h). These differences in magnitude between the cyclone composites in the 850 hPa earth-relative wind speeds, which would occur at an altitude of approximately 1 km above the surface, are also shown when analysing the composite 10-metre earth-relative wind speeds per cyclone class (see Figure S3 in the supplementary material). Overall, the

210 North Atlantic Ocean winter extra-tropical cyclone composite has the strongest 10-metre wind speeds, and the Arctic summer cyclone composite has the weakest 10-metre wind speeds. This is likely a consequence of the weaker pressure gradients within the Arctic summer cyclone composite.

  In each cyclone composite, the maximum 850 hPa earth-relative wind speeds occur in the southern region of the composite and near the composite centre (see Figure 3b, 3e and 3h). Earth-relative winds are the combination of the cyclones

215 system-relative winds and the cyclones propagation velocity. The cyclone composite 850 hPa earth-relative winds are highest in this region, because the cyclonic (anti-clockwise) system-relative winds and the cyclones propagation direction are in the same direction. Therefore the 850 hPa system-relative winds are enhanced by the propagation velocity, thus resulting in the highest earth-relative 850 hPa in the southern region of the cyclone composites. The area where the 850 hPa earth-relative wind speeds exceed 10 m s^{-1} is also much greater in the Arctic winter and North Atlantic Ocean extra-tropical cyclone

220 composites than the Arctic summer cyclone composite (see Figure 3b, 3e and 3h).
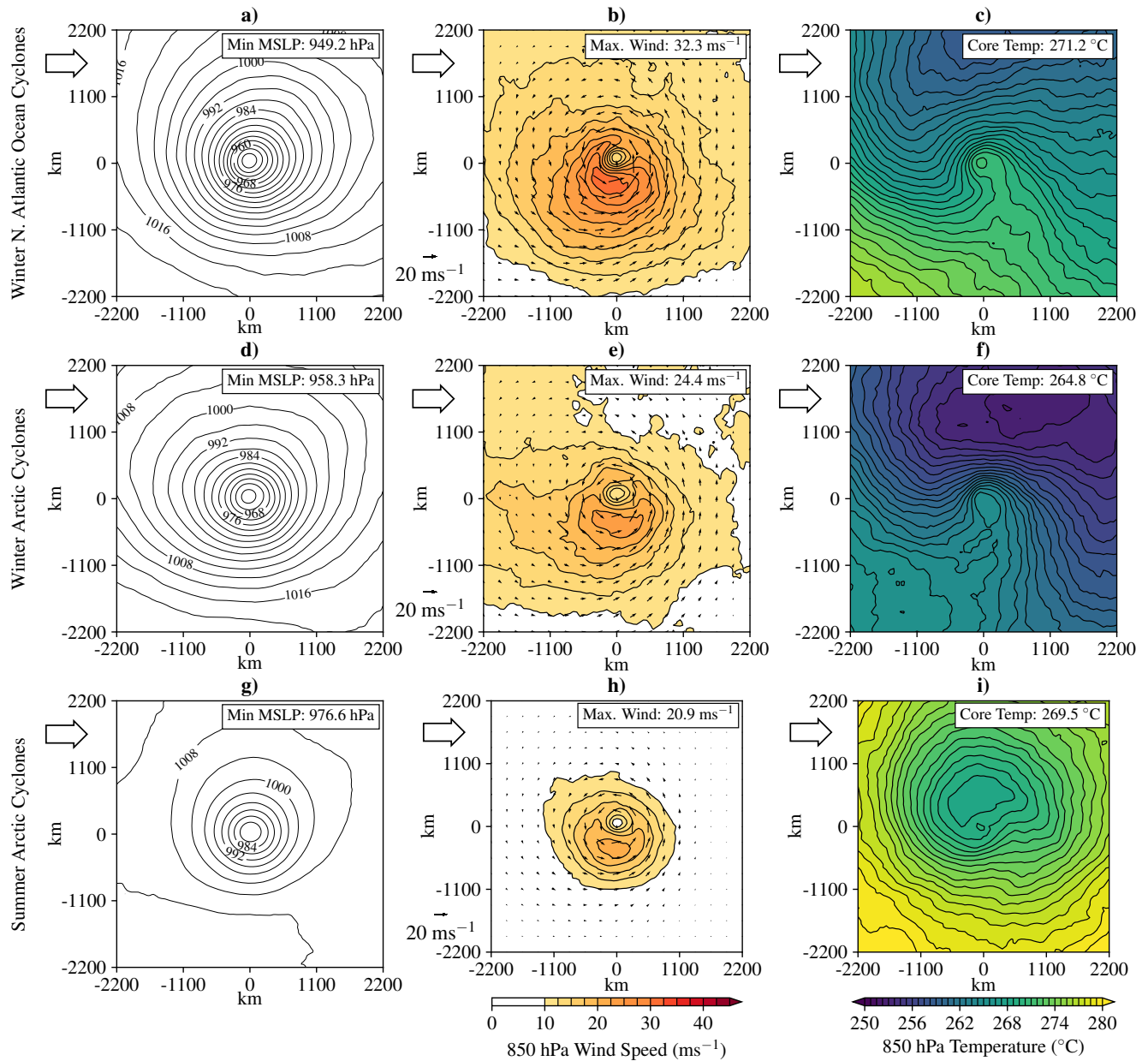
Figure 3. Horizontal mean sea level pressure (MSLP) (hPa) (left panel), 850 hPa earth-relative wind speed (m s^{-1}) (middle panel) and 850 hPa temperature (°C) (right panel) composite structure at the time of maximum intensity (minimum MSLP), of winter (DJF) North Atlantic Ocean extra-tropical cyclones (top panel), winter Arctic cyclones (middle panel), and summer (JJA) Arctic cyclones (bottom panel). The large arrow indicates the direction of storm propagation.

Despite similarities in the spatial distribution of the 850 hPa earth-relative winds within each composite, the 850 hPa temperature structure of the Arctic summer cyclone composite is different to that of the winter Arctic and North Atlantic Ocean extra-tropical cyclone composites (see Figure 3c, 3f and 3i). At the time of maximum intensity, the Arctic summer cyclone composite is characterised by a cold core at the centre of the composite (see Figure 3i). In contrast, the winter Arctic and North Atlantic Ocean extra-tropical cyclone composites are characterised by high temperature gradients between the warm air below and cold air above the composite cyclone centres (see Figure 3c and 3f). These divisions between warm and cold air would be associated with the location of weather fronts. The winter Arctic and North Atlantic Ocean extra-tropical cyclone composites also show signs that cold air has started to occlude into the warm air around the composite cyclone centre.

The 850 hPa temperature structure of the Arctic summer cyclone composite is different to the winter Arctic cyclone and North Atlantic Ocean winter extra-tropical cyclone composites. It is also different to that described in the Norwegian Cyclone Model and Shapiro-Keyser Model (Bjerknes, 1919, 1922; Shapiro and Keyser, 1990). This contrasts with results from Clancy et al. (2022), who show that the structure of Arctic cyclones in every season is comparable to those in the mid-latitudes. However, Clancy et al. (2022) used a different cyclone compositing methodology, storm tracking algorithm that is applied to different reanalysis datasets (ERA-Interim and NCEP/NCAR reanalyses rather than ERA-5) and metric of intensity to obtain the most intense cyclones. Clancy et al. (2022) also did not filter Arctic cyclones to retain the 100 most intense cyclones per season, instead calculating the cyclone composite as an average of thousands more cyclones per season, which may smooth out this unique axi-symmetric structure of Arctic summer cyclone composites (see Figure 3).

3.4 Vertical composite structure at the time of maximum intensity

Cyclones typically contain conveyor belts, which are distinct airstreams occurring in different regions and altitudes within a cyclone (Browning, 1997; Catto et al., 2010; Dacre et al., 2012). These include a warm conveyor belt (WCB) that is typically located in front of the cold front and ascends from south to north parallel to the front. The WCB typically rises above the cold conveyor belt (CCB), which typically occurs at low-levels in the atmosphere and wraps around above the cyclone centre (Browning, 1997).

The ascent of air associated with the WCB is shown in the winter North Atlantic Ocean extra-tropical cyclone and the Arctic winter cyclone composites ahead of the cyclone centre where the cold front would typically be located (see Figure 4a, 4b and 4c). This suggests that a WCB may be present within each composite. In the Arctic summer cyclone composite, the magnitude of ascent shown in the vertical velocity composite is much weaker than in the winter North Atlantic Ocean extra-tropical cyclone and Arctic cyclone composites (see Figure 4). The maximum vertical velocity in the winter North Atlantic Ocean extra-tropical cyclone composite is 28.7 hPa h^{-1}, 17.2 hPa h^{-1} in the Arctic winter cyclone composite, and 9.6 hPa h^{-1} in the Arctic summer cyclone composite (see Figure 4). This suggests that the WCB may be less well defined in Arctic summer cyclones.

The 400 hPa relative humidity composites for each class of cyclone show that the Arctic summer cyclone composite is more axi-symmetric than the winter North Atlantic Ocean extra-tropical cyclone composite and the Arctic winter cyclone composite (see Figure 4d, 4e and 4f). High values of relative humidity are more confined around the composite cyclone centre (above
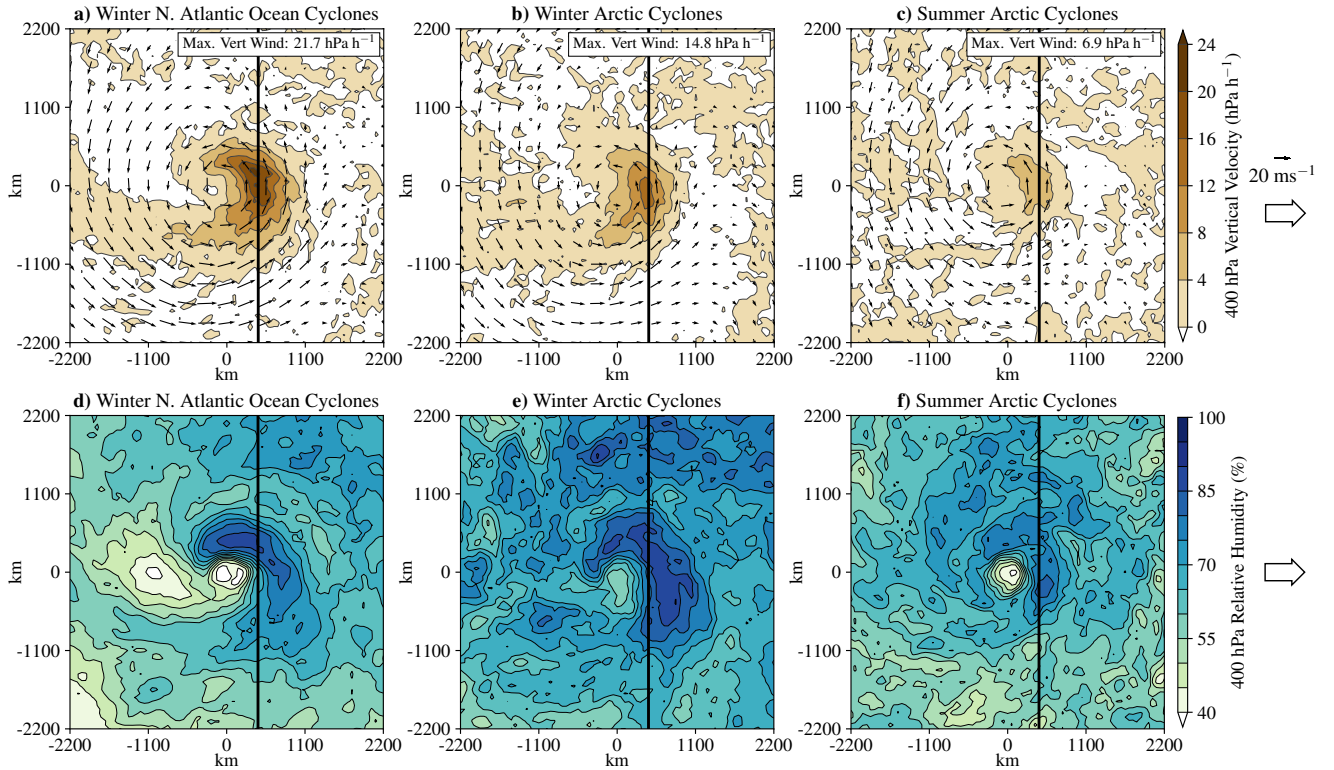
Figure 4. Horizontal 400 hPa system relative winds (m s^{-1}) (quivers) and vertical velocity (hPa h^{-1}) (contours) (top panel), and 400 hPa relative humidity (%) (bottom panel) composite structure at the time of maximum intensity (minimum MSLP), of winter (DJF) North Atlantic Ocean extra-tropical cyclones (left panel), winter Arctic cyclones (middle panel), and summer (JJA) Arctic cyclones (right panel). Positive values of vertical velocity indicate ascent. The large arrow indicates the direction of storm propagation. The transect (bold line) 4° degrees ahead of the composite cyclone centre and perpendicular to the cyclones direction of propagation indicates the vertical slice used to produce Fig. 5.

and to the right) in the North Atlantic Ocean extra-tropical cyclone and Arctic winter cyclone composites, perhaps indicating where moisture has risen from the surface within the cyclone at the typical location of weather fronts. West of the composite cyclone centre, drier air is shown at the 400 hPa level in the North Atlantic Ocean extra-tropical cyclone composite that appears to be intruding towards the composite cyclone centre, perhaps indicating the presence of a dry intrusion. But this feature is less pronounced in the winter and summer Arctic cyclone composites.

By analysing the transect outlined in Figure 4, the CCB appear to be present in both the winter Arctic and North Atlantic Ocean cyclone composites (see Figure 5a and 5b). The CCB is shown by the low-level high magnitude system-relative zonal (U-component) wind speeds within the vertical cross section, which occur approximately 550 km above the composite cyclone centre. The magnitude of the zonal winds of the CCB are lower in the Arctic winter cyclone composite (approximately 18 m
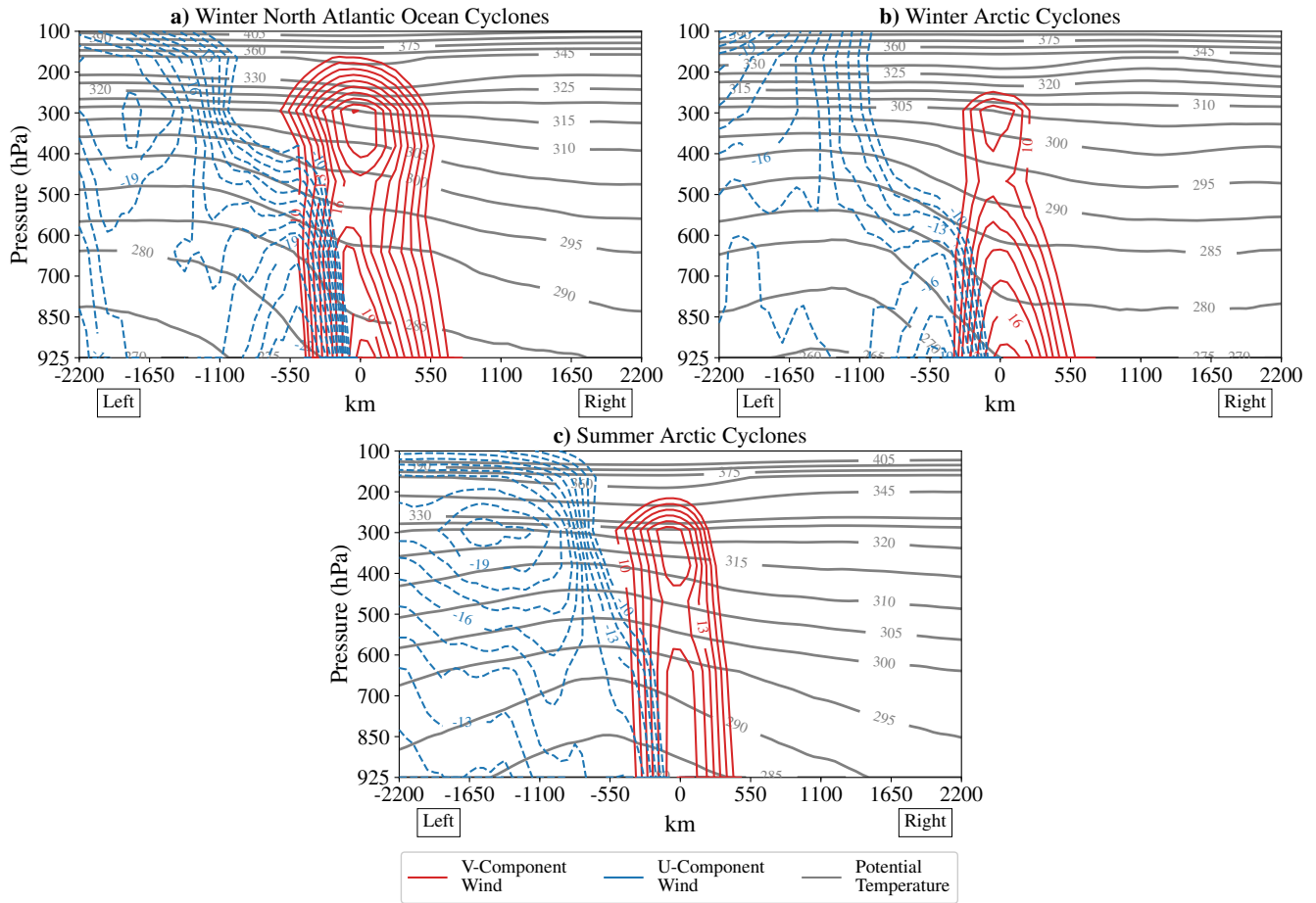
Figure 5. Composite vertical slices through the transect perpendicular to the direction of cyclone propagation and 4° ahead of the composite cyclone centre (see Figure 4), of **a)** winter (DJF) North Atlantic Ocean extra-tropical cyclones, **b)** winter Arctic cyclones, and **c)** summer (JJA) Arctic cyclones. Red contours (shown every 1 m s^{-1} from 10 m s^{-1}) show the V-component (meridional) winds, blue contours (shown every 1.0 m s^{-1} below -10 m s^{-1}) show the U-component (zonal) winds and grey contours (shown every 5 °C up to 330 °C and then every 15 °C) show potential temperature isentropes. The positions (left / right) are shown relative to the cyclone propagation direction.

s^{-1}) than the North Atlantic Ocean winter cyclone composite (approximately 22 m s^{-1}). But in the Arctic summer cyclone composite, the highest zonal wind speeds above the cyclone composite centre do not occur at the surface (see Figure 5c). Instead, the highest zonal wind speeds occur at the 300 hPa level approximately 1600 km from the cyclone composite centre. This suggests that the CCB, which typically occurs near the surface, is less well defined in summer Arctic cyclones.

The WCB is shown in the winter Arctic and North Atlantic Ocean cyclone composites by the high magnitude meridional (V-component) system-relative winds within the vertical cross section, which occur south of the CCB and between 925 hPa to 600 hPa (see Figure 5a and 5b). Like the CCB, the maximum magnitude of these meridional wind speeds is lower in the Arctic

winter cyclone composite (approximately 18 m s^{-1}) than the North Atlantic Ocean winter cyclone composite (approximately 20 m s^{-1}). The spatial distribution of the system-relative wind speeds in these composites is similar to that shown by Catto et al. (2010), who showed the composite structure of the 50 most intense North Atlantic and Pacific Ocean extra-tropical cyclones, using the ERA-40 reanalysis dataset. The stark changes in the wind direction shown above the cyclone composite centre in each cross section of the winter North Atlantic Ocean cyclone and Arctic cyclone composites indicates the presence of the CCB and WCB in each composite.

The distribution of the potential temperature isentropes within the Arctic summer cyclone composite cross section also differs to that of winter Arctic and North Atlantic Ocean extra-tropical cyclones (see Figure 5). In contrast, the slope of the potential temperature isentropes reverses above the composite cyclone centre, where the isentropes ascend but then descend below and above the cyclone composite centre along this cross section (see Figure 5c). At the time of maximum intensity, Arctic summer cyclones have developed a cold core (see Figure 3), which could contribute to this distribution in the isentropes.

3.5 Development in the horizontal composite structure

The 700 hPa temperature structure of the winter North Atlantic Ocean extra-tropical cyclone composite and the winter and summer Arctic cyclone composites 48 hours before the time of maximum intensity is similar, with each cyclone developing in a region of high temperature gradients (see Figure 6). This is similar to the Polar Front described by Bjerknes (1919, 1922). Temperature gradients within the winter North Atlantic Ocean extra-tropical cyclone and Arctic cyclone composites are much greater than that of the summer Arctic cyclone composite. This is likely because intense winter Arctic cyclones also tend to develop over the North Atlantic Ocean (see Figure 2), where meridional temperature gradients and baroclinicity are high, especially in winter (Serreze et al., 2001). However, from the time of maximum intensity, the development in the Arctic summer cyclone composite differs to that of the winter North Atlantic Ocean extra-tropical cyclone and Arctic cyclone composites.

After the time of maximum intensity, the Arctic summer cyclone composite develops a cold core centre that becomes more defined and colder (see Figures 6i and 7). The temperature anomaly at the composite cyclone centre at the time of maximum intensity is -3.8 °C (see Figure 6h), but lowers to -8.7 °C and -10.6 °C 48 and 144 hours after the time of maximum intensity (see Figures 6i and 7b). This shows that Arctic summer cyclones tend to develop a cold core centre around the time of maximum intensity and retain this structure until they dissipate.

This is in contrast with the winter Arctic and North Atlantic Ocean extra-tropical cyclone composites that appear to follow the process of occlusion, where cold air wraps around the composite centre (see Figure 6). This structural transition of the Arctic summer cyclone composite is also different to the Norwegian Cyclone Model (Bjerknes, 1919, 1922), where cyclones tend to undergo occlusion, and the Shapiro-Keyser Model (Shapiro and Keyser, 1990), where cyclones tend to undergo frontal fracture and develop a warm core centre.

3.6 Development in the vertical composite structure

The unique structural transition in temperature of the Arctic summer cyclone composite is also shown throughout the vertical extent of the composite (see Figure 8). From the time of maximum intensity, cold air in the Arctic summer cyclone composite
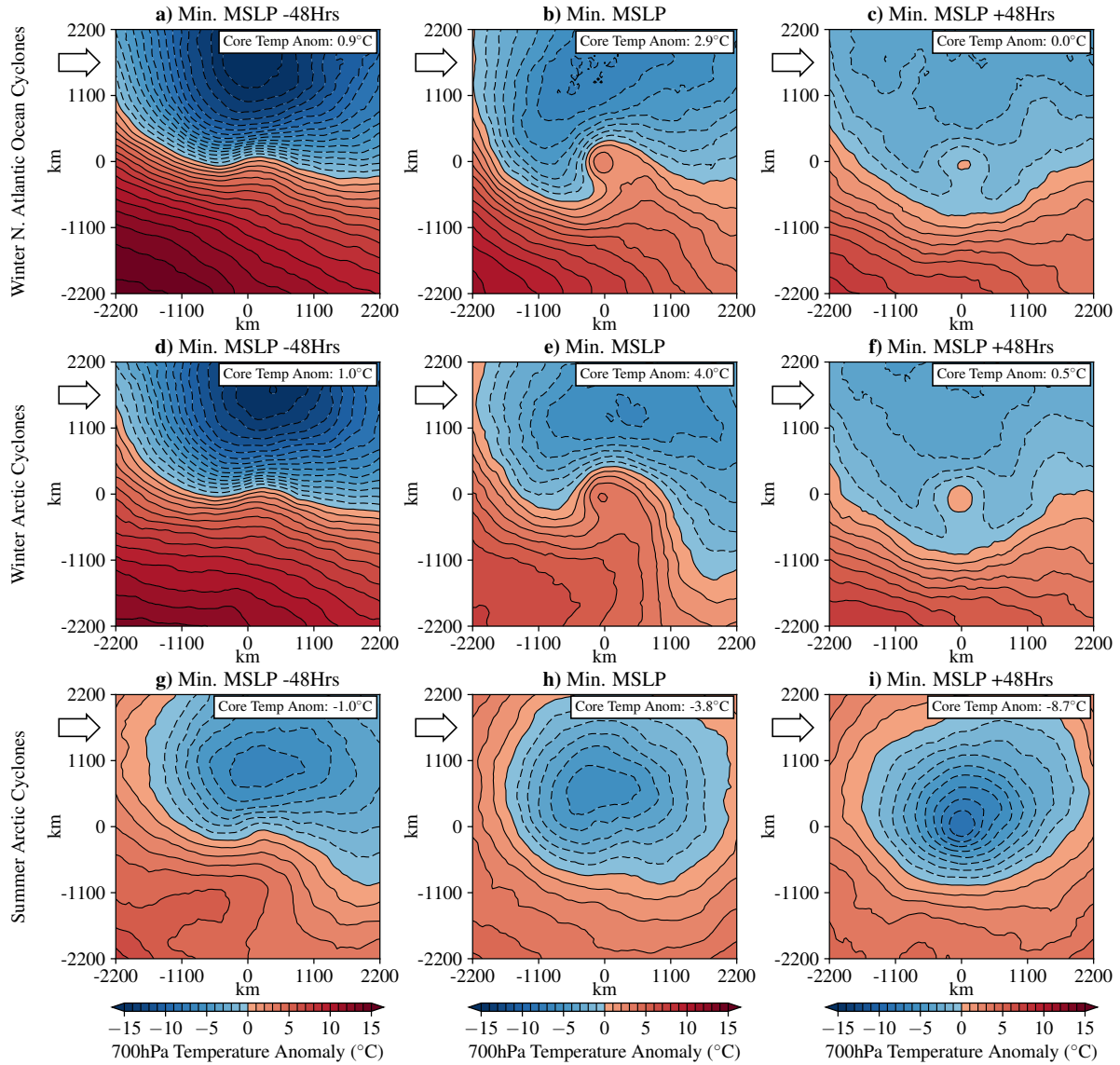
Figure 6. Horizontal 700 hPa temperature anomaly (°C) composite structure 48 hours before the time of maximum intensity (minimum MSLP) (left panel), **b)** at the time of maximum intensity (middle panel), and 48 hours after the time of maximum intensity (right panel), of winter (DJF) North Atlantic Ocean extra-tropical cyclones (top panel), winter Arctic cyclones (middle panel), and summer (JJA) Arctic cyclones (bottom panel). The large arrow indicates the direction of storm propagation.

appears to intrude through the centre of the composite, which ultimately leads to the composite developing a cold core structure
305 throughout the troposphere (see Figure 8g, 8h and 8i). This is similar to the structure found in 'The Great Arctic Cyclone of 2012', which was shown by Aizawa and Tanaka (2016).
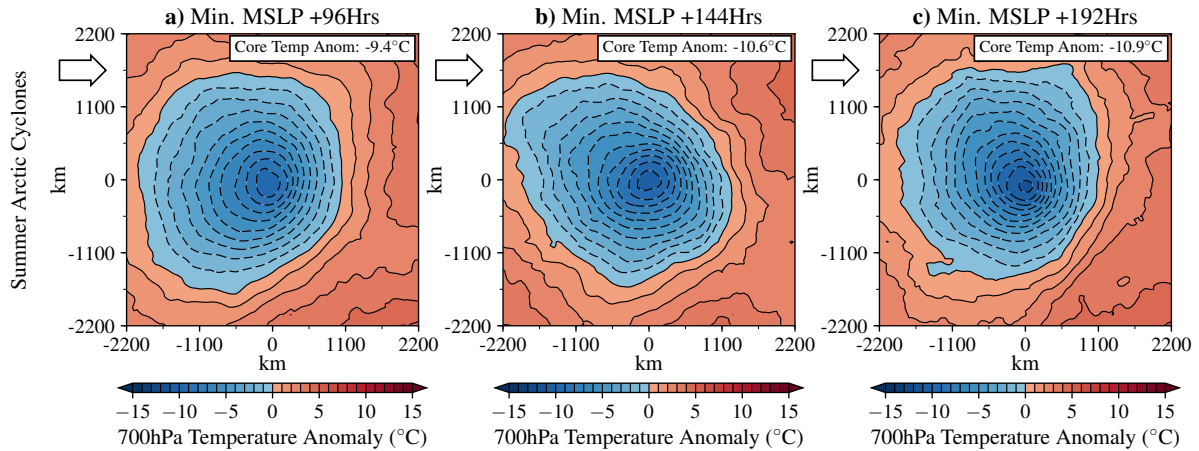
Figure 7. Horizontal 700 hPa temperature anomaly (°C) composite structure 96 (left), 144 (middle) and 192 (right) hours after the time of maximum intensity (minimum MSLP) of summer (JJA) Arctic cyclones. The large arrow indicates the direction of cyclone propagation.

The temperature anomaly in the stratosphere is also much more defined and larger (8.0 - 9.0 °C) in the Arctic summer cyclone composite at and after the time of maximum intensity (see Figure 8h and 8i). In contrast, the maximum temperature anomaly in the stratosphere after the time of maximum intensity in the winter North Atlantic Ocean extra-tropical cyclone and Arctic cyclone composites is 5.0 - 6.0 °C (see Figure 8). Furthermore, the altitude of the tropopause is much lower in the Arctic summer cyclone composite at and after the time of maximum intensity than the winter North Atlantic Ocean extra-tropical cyclone and Arctic cyclone composites (see Figure 8). The level of tropopause is shown to be approximately 500 hPa at the centre of Arctic summer cyclone composite at and after the time of maximum intensity. In contrast, the level of tropopause is approximately 300 hPa at the centre of the winter North Atlantic Ocean extra-tropical cyclone and Arctic cyclone composites at and after the time of maximum intensity. These differences suggest that the development of intense Arctic summer cyclones may be more influenced by the stratosphere than intense winter Arctic and North Atlantic Ocean cyclones.

The vertical temperature structure of the Arctic summer cyclone composite is shown to be more axi-symmetric from the time of maximum intensity than the winter North Atlantic Ocean cyclone and winter Arctic cyclone composites (see Figure 8). This axi-symmetric structure after the time of maximum intensity is also shown in the system-relative wind speed fields (see Figure 9). After 48 hours from the time of maximum intensity, the Arctic summer cyclone composite develops system zonal and meridional system-relative winds around the composite cyclone centre, with a of similar magnitude each side of the composite cyclone (see Figure 9c and Figure 9f). Notably, system-relative winds are lower near the surface than in the upper atmosphere, where human activity would tend to occur.
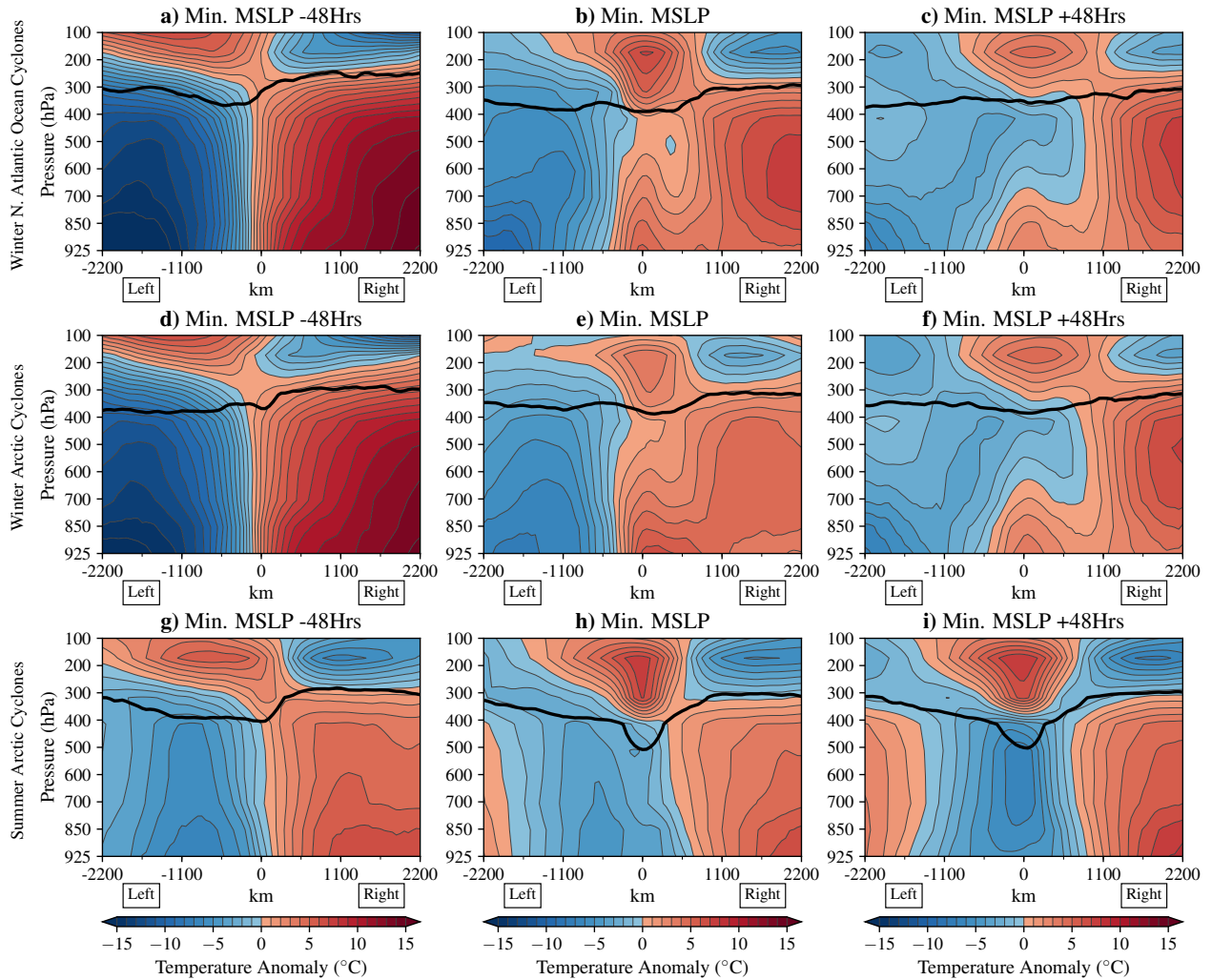
Figure 8. Vertical temperature anomaly (°C) composite of winter (DJF) North Atlantic Ocean extra-tropical cyclones (top panel), winter Arctic cyclones (middle panel), and summer (JJA) Arctic cyclones (bottom panel), along the transect perpendicular to the cyclone propagation direction through the composite cyclone centre, 48 hours before the time of maximum intensity (i.e., minimum MSLP) (left panel), at the time of maximum intensity (middle panel), and 48 hours after the time of maximum intensity (right panel). The thick black contour indicates the level of the tropopause (i.e., the 2PVU contour). The positions (left / right) are shown relative to the cyclone propagation direction.

3.7 Comparison of the Arctic summer cyclone composite to the Aizawa and Tanaka (2016) model

325   Aizawa and Tanaka (2016) proposed a conceptual model of the structure of Arctic summer cyclones, based on just two past Arctic summer cyclone case studies. Here, the composite structure of the 100 most intense Arctic summer cyclones has been determined, allowing for the evaluation of the Aizawa and Tanaka (2016) conceptual model to the composite structure of a
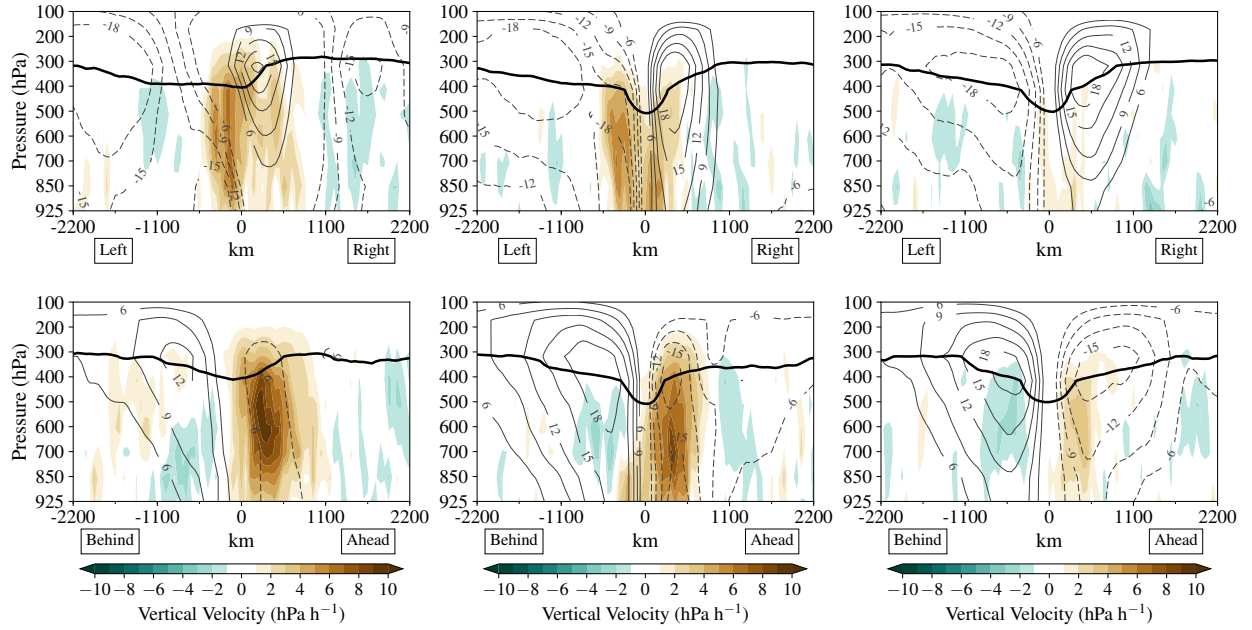
Figure 9. Vertical velocity (hPa h^{-1}) (colour) and system-relative (m s^{-1}) U-component (zonal) and V-component (meridional) wind speed (contours) composite structure of the 100 most intense summer (JJA) Arctic cyclones, (top panel) along the transect perpendicular to the cyclone propagation direction through the composite cyclone centre and (bottom panel) along the transect parallel to the cyclone propagation direction through the composite cyclone centre. Positive values of vertical velocity indicate ascent. Composites are shown 48 hours before the time of maximum intensity (i.e., minimum mean sea level pressure (MSLP) (left panel), at the time of maximum intensity (middle), and 48 hours after the time of maximum intensity (right panel). The thick black contour indicates the level of the tropopause (i.e., the 2PVU contour).

greater sample of past intense Arctic summer cyclones. This conceptual model highlights six main features of Arctic summer cyclones, which include: a warm core in the lower stratosphere and cold core in the troposphere, a deep tropopause fold descending down to 500 hPa over the cyclone centre, a secondary circulation in the troposphere, a downdraft in the lower stratosphere and a deep cyclonic circulation up into the stratosphere. Aizawa and Tanaka (2016) also describe Arctic summer cyclones as being one of the largest cyclones found on the Earth, with a horizontal diameter of 5,000 km at upper levels (i.e., in the stratosphere).

There are similarities between the Arctic summer cyclone composite and this conceptual model. The composite vertical structure of Arctic summer cyclones shows a warm anomaly in the lower stratosphere (up to 100 hPa) and a cold core throughout the troposphere (see Figure 8). There is also a deep tropopause fold that descends to 500 hPa shown in the Arctic summer cyclone composite (see Figure 8).

Despite these similarities, the Arctic summer cyclone composites does also show differences to the Aizawa and Tanaka (2016) model. The general size of the Arctic summer cyclone composite appears to be smaller near the surface than the winter

340   Arctic and North Atlantic Ocean cyclone composites (see Figure 3). This is implied by the area within the last-closed isobar (see Figure 3a, 3d and 3g), and the area within the 10 m s^{-1} earth-relative wind speed contour of each cyclone composite (see Figure 3b, 3e and 3h). Although Aizawa and Tanaka (2016) use a different metric to infer cyclone size, the Arctic summer cyclone composite is smaller in size than the winter Arctic and North Atlantic Ocean cyclone composites near the surface. In this study, cyclone size is inferred by the area within the last closed isobar and the area where the 850 hPa earth-relative wind

345   speeds exceed 10 m s^{-1} (see Figure 3 and Section 3.3).

    The Arctic summer cyclone composite from the time of maximum intensity also does not show a secondary circulation in the troposphere or deep cyclonic circulation into the stratosphere or a downdraft in the stratosphere (Figure 9). Before and after the time of maximum intensity, the Arctic summer cyclone composite does not show downdrafts (negative vertical velocity) on the outer flanks of the composite (see Figure 9). Only weak (> -3.0 hPa h^{-1}) downdrafts are shown in the composite before

350   and at the time of maximum intensity (see Figure 9).

    Overall, by analysing the composite structure of a large sample of past Arctic summer cyclones, there is evidence to support some aspects of the Aizawa and Tanaka (2016) conceptual model. Results from this study show that after the time of maximum intensity, intense Arctic summer cyclones do indeed likely have a warm core in the lower stratosphere and a cold core throughout the troposphere, and a deep tropopause fold descending into the troposphere over the cyclone centre.

355   However, there is insufficient evidence in this study to suggest that typical intense Arctic summer cyclones have a secondary circulation in the troposphere, a downdraft in the lower stratosphere, a deep cyclonic circulation up into the stratosphere and a horizontal extent of approximately 5,500 km (typical Arctic summer cyclones are likely smaller).

    An aspect that is highlighted in this study, is that intense Arctic summer cyclones appear to typically undergo a structural transition during their lifecycle. The development in the composite structure of intense Arctic summer cyclones shows that

360   they undergo a transition from having a baroclinic structure to an axi-symmetric cold core structure throughout the troposphere around the time of maximum intensity. After this transition, the structure of intense Arctic summer cyclones is somewhat similar to the Aizawa and Tanaka (2016) model. Aizawa and Tanaka (2016) showed this structural transition when analysing 'The Great Arctic Cyclone of 2012' and for another Arctic summer cyclone in June 2008. The composite Arctic summer cyclone shown in this study suggests that this transition has likely occurred in other past intense Arctic summer cyclones and

365   that it may be typical of intense Arctic summer cyclones.

4   Summary and Conclusions

The location and intensity of hazardous weather within a cyclone is dependent on its development and structure. Previous analysis of individual past Arctic summer cyclones suggests that they may have a different structure to typical extra-tropical cyclones (e.g., Tanaka et al., 2012; Aizawa et al., 2014; Aizawa and Tanaka, 2016; Tao et al., 2017). However, these previous

370   studies only focused on individual case studies, therefore the generality in the development and structure of Arctic cyclones has not yet been determined.

This study aims to describe the typical lifetime, structure, and development of a large sample of past intense Arctic cyclones, using a storm compositing methodology. The composite structure of the 100 most intense summer (JJA) and winter (DJF) Arctic cyclones is compared with that of the 100 most intense extra-tropical winter cyclones occurring over the North Atlantic Ocean between 1979-2020, using data from the ERA-5 reanalysis dataset. Overall, this study shows that Arctic summer cyclones are typically longer lived and have a different development in their composite structure to winter Arctic and North Atlantic Ocean extra-tropical cyclones, and to that described in conceptual models such as the Norwegian Cyclone Model (Bjerknes, 1919, 1922) and the Shapiro Keyser Model (Shapiro and Keyser, 1990).

  – Intense Arctic summer cyclones have longer lifetimes than winter Arctic and North Atlantic Ocean extra-tropical cyclones.

Cyclones are associated with hazardous weather, including high wind speeds and high ocean waves (Thomson and Rogers, 2014; Liu et al., 2016; Waseda et al., 2018; Squire, 2020; Waseda et al., 2021). Arctic cyclones can also enhance the break-up sea ice, which may then become mobile and drift toward shipping lanes, creating an additional hazard to shipping, oil exploration and tourism activities (Simmonds and Keay, 2009; Asplin et al., 2012; Parkinson and Comiso, 2013; Peng et al., 2021). It is found that Arctic summer cyclones are typically much longer lived than winter Arctic and North Atlantic Ocean extra-tropical cyclones. The mean lifetime of the 100 most intense Arctic summer cyclones is found to be more than 3 days longer than that of the 100 most intense winter Arctic and North Atlantic Ocean extra-tropical cyclones. Consequently, Arctic summer cyclones may cause prolonged hazardous weather conditions and prolonged disruption to human activities in the Arctic.

  – The development shown in the composite structure of intense Arctic summer cyclones is different to that of winter Arctic and North Atlantic Ocean extra-tropical cyclones, and to the description given in conceptual models such as the Norwegian Cyclone Model (Bjerknes, 1919, 1922) and Shapiro-Keyser Model (Shapiro and Keyser, 1990).

The development shown in the composite structure of the 100 most intense Arctic summer cyclones shows that they typically undergo a transition from a baroclinic structure to an axi-symmetric cold core structure throughout the troposphere around the time of maximum intensity (i.e., the time of minimum MSLP). This axi-symmetric cold core structure is consistent with previous studies that have analysed past individual Arctic summer cyclone case studies (Tanaka et al., 2012; Aizawa et al., 2014; Aizawa and Tanaka, 2016; Tao et al., 2017). In comparison, the composite structure of the 100 most intense winter Arctic cyclones is similar to that of the 100 most intense North Atlantic Ocean extra-tropical cyclones, with both of the cyclone composites showing a baroclinic structure with high meridional temperature gradients and signs of occlusion throughout their lifecycle. From the time of maximum intensity, the Arctic summer cyclone composite has a much lower-lying tropopause and a larger positive temperature anomaly in the stratosphere at the centre of the cyclone composite than the winter Arctic and North Atlantic Ocean extra-tropical cyclone composites. The Arctic summer cyclone composite retains this axi-symmetric cold core structure long after the time of maximum intensity.

The composite structural development of Arctic summer cyclones is found to be different to that of winter North Atlantic Ocean extra-tropical cyclones and winter Arctic cyclones. This is also different to the structural development of extra-tropical

cyclones described in the Norwegian Cyclone Model (Bjerknes, 1919, 1922) and Shapiro-Keyser Model (Shapiro and Keyser, 1990). The Arctic summer cyclone composite also shows differences to the Arctic Cyclone Model proposed by Aizawa and Tanaka (2016). This raises questions such as whether this unique structural transition of Arctic summer cyclones is captured in climate model projections and weather forecasting models, and how might the frequency of these Arctic summer cyclones change in response to climate change?

The results found in this study contrast with those in Clancy et al. (2022), who show that the structure of Arctic cyclones in all seasons is similar to mid-latitude cyclones. However, there are numerous differences in the methods between this study and Clancy et al. (2022). In this study, cyclone composites were calculated across the 100 most intense cyclones per season, but in Clancy et al. (2022), thousands more cyclones were included when producing cyclone composites. It is possible that this unique structural development of Arctic summer cyclones is only present in the most intense Arctic summer cyclones, and why it was shown in this study and not in Clancy et al. (2022). In addition, Clancy et al. (2022) use a different cyclone compositing method, storm tracking algorithm applied to different reanalysis datasets, and a different intensity metric to determine the most intense cyclones that contribute to their composites. These differences in method may also contribute to the differences with the results presented in this study. Future work may seek to test the sensitivity of sample size and composite method on determining the structure of intense Arctic cyclones.

It is plausible that the structural transition of Arctic summer cyclones, which don't fully undergo occlusion, may contribute to extending the lifetimes of such cyclones. Arctic summer cyclones may lack the dynamical forcing from the occlusion process that typically helps to force the movement of air that leads to the dissipation of extra-tropical cyclones. The Arctic summer cyclone composite is also found to have a lower tropopause and greater temperature anomaly in the stratosphere at the centre than the winter Arctic and North Atlantic Ocean extra-tropical cyclone composites. This suggests that they may be more strongly influenced by the stratosphere and, in particular, Tropopause Polar Vortices (TPVs) that are common features based on the tropopause in the Arctic (Cavallo and Hakim, 2010). Recent studies have suggested that some Arctic cyclones may have been strongly influenced by TPVs (e.g., Simmonds and Rudeva, 2014; Tao et al., 2017; Gray et al., 2021). Understanding what causes this structural transition of Arctic summer cyclones and why they tend to have longer lifetimes than winter Arctic and extra-tropical cyclones is an area for future research.

Data availability. Data sets for this research are available in these in-text data citation references and the associated repositories. ERA5 reanalysis data (Hersbach et al., 2020). The TRACK algorithm is available on the University of Reading's Git repository (GitLab) at https://gitlab.act.reading.ac.uk/track/track2021 (Hodges, 2021).

Author contributions. Alexander F. Vessey conducted all of the analysis detailed in this paper and took responsibility to write this paper. Kevin I. Hodges, Len C. Shaffrey and Jonathan J. Day assisted with this analysis and writing.

Competing interests. The contact author has declared that neither they nor their co-authors have any competing interests.

Acknowledgements. The authors acknowledge the funding and support from the Scenario NERC Doctoral Training Partnership Grant (NE/L002566/1) and co-sponsor, AXA XL, in the development of this research. The authors would also like to acknowledge the European Centre for Medium-Range Weather Forecasts (ECMWF) for the production of ERA-5 reanalysis dataset. The work described in this paper

440   has received funding from the European Union's Horizon 2020 Research and Innovation programme through Grant agreement no. 727862 APPLICATE. The content of the article is the sole responsibility of the author(s) and it does not represent the opinion of the European Commission, and the Commission is not responsible for any use that might be made of information contained. Finally, we thank the anonymous reviewers for their constructive comments that helped to improve this manuscript.

References

445 Aizawa, T. and Tanaka, H.: Axisymmetric structure of the long lasting summer Arctic cyclones, Polar Sci., 10, 192–198, 2016.

Aizawa, T., Tanaka, H., and Satoh, M.: Rapid development of Arctic cyclone in June 2008 simulated by the cloud resolving global model NICAM, Meteorol. Atmos. Phys., 126, 105–117, 2014.

Årthun, M., Onarheim, I. H., Dörr, J., and Eldevik, T.: The seasonal and regional transition to an ice-free Arctic, Geophysical Research Letters, 48, e2020GL090 825, 2021.

450 Asplin, M. G., Galley, R., Barber, D. G., and Prinsenberg, S.: Fracture of summer perennial sea ice by ocean swell as a result of Arctic storms, J. Geophys. Res.: Oceans, 117, 2012.

Babin, J., Lasserre, F., and Pic, P.: Arctic shipping and polar seaways, Encyclopedia of water: science, technology, and society, 2020.

Bauer, M. and Del Genio, A. D.: Composite analysis of winter cyclones in a GCM: Influence on climatological humidity, Journal of climate, 19, 1652–1672, 2006.

455 Bengtsson, L., Hodges, K. I., Esch, M., Keenlyside, N., Kornblueh, L., Luo, J.-J., and Yamagata, T.: How may tropical cyclones change in a warmer climate?, Tellus, 59, 539–561, 2007.

Bengtsson, L., Hodges, K. I., and Keenlyside, N.: Will extra-tropical storms intensify in a warmer climate?, J. Clim., 22, 2276–2301, 2009.

Bjerknes, J.: On the structure of moving cyclones, Mon. Weather Rev., 47, 95–99, 1919.

Bjerknes, J.: Life cycle of cyclones and the polar front theory of atmospheric circulation, Geophys. Publik., 3, 1–18, 1922.

460 Browning, K.: The dry intrusion perspective of extra-tropical cyclone development, Meteor. Appl., 4, 317–324, 1997.

Browning, K.: The sting at the end of the tail: Damaging winds associated with extra-tropical cyclones, Q. J. R. Meteorol. Soc., 130, 375–399, 2004.

Carlson, T. N.: Airflow through mid-latitude cyclones and the comma cloud pattern, Mon. Weather Rev., 108, 1498–1509, 1980.

Catto, J. L., Shaffrey, L. C., and Hodges, K. I.: Can climate models capture the structure of extra-tropical cyclones?, J. Clim., 23, 1621–1635,
465 2010.

Catto, J. L., Madonna, E., Joos, H., Rudeva, I., and Simmonds, I.: Global relationship between fronts and warm conveyor belts and the impact on extreme precipitation, Journal of Climate, 28, 8411–8429, 2015.

Cavallo, S. M. and Hakim, G. J.: Composite structure of tropopause polar cyclones, Mon. Weather Rev., 138, 3840–3857, 2010.

Clancy, R., Bitz, C. M., Blanchard-Wrigglesworth, E., McGraw, M. C., and Cavallo, S. M.: A cyclone-centered perspective on the drivers of
470 asymmetric patterns in the atmosphere and sea ice during Arctic cyclones, Journal of Climate, 35, 73–89, 2022.

Crawford, A. D. and Serreze, M. C.: Does the summer Arctic frontal zone influence Arctic Ocean cyclone activity?, J. Clim., 29, 4977–4993, 2016.

Dacre, H.: A review of extra-tropical cyclones: observations and conceptual models over the past 100 years, Weather, 75, 4–7, 2020.

Dacre, H., Hawcroft, M., Stringer, M., and Hodges, K.: An extra-tropical cyclone atlas: A tool for illustrating cyclone structure and evolution
475 characteristics, Bull. Am. Meteorol. Soc., 93, 1497–1502, 2012.

GISTEMP Team: GISS Surface Temperature Analysis (GISTEMP), version 4, pp. Accessed 17 Jun 2021, https://data.giss.nasa.gov/gistemp/, 2021.

Gray, S. L., Hodges, K. I., Vautrey, J. L., and Methven, J.: The role of tropopause polar vortices in the intensification of summer Arctic cyclones, Weather and Climate Dynamics, pp. 1–31, 2021.

480 Harsem, Ø., Heen, K., Rodrigues, J., and Vassdal, T.: Oil exploration and sea ice projections in the Arctic, The Polar Record, 51, 91, 2015.

Hersbach, H., Bell, B., Berrisford, P., Hirahara, S., Horányi, A., Muñoz-Sabater, J., Nicolas, J., Peubey, C., Radu, R., Schepers, D., et al.: The ERA5 global reanalysis, Q. J. R. Meteorol. Soc., 146, 1999–2049, 2020.

Hodges, K. I.: A general method for tracking analysis and its application to meteorological data, Mon. Weather Rev., 122, 2573–2586, 1994.

Hodges, K. I.: Feature tracking on the unit sphere, Mon. Weather Rev., 123, 3458–3465, 1995.

485   Hodges, K. I.: Adaptive constraints for feature tracking, Mon. Weather Rev., 127, 1362–1373, 1999.

Hodges, K. I.: TRACK tracking and analysis system for weather, climate and ocean data, Gitlab [code], pp. Accessed 09 Nov 2020, https://gitlab.act.reading.ac.uk/track/track2021, 2021.

Leckebusch, G. C., Ulbrich, U., Fröhlich, L., and Pinto, J. G.: Property loss potentials for European midlatitude storms in a changing climate, Geophys. Res. Lett., 34, 2007.

490   Lenssen, N. J., Schmidt, G. A., Hansen, J. E., Menne, M. J., Persin, A., Ruedy, R., and Zyss, D.: Improvements in the GISTEMP uncertainty model, J. Geophys. Res.: Atmos., 124, 6307–6326, 2019.

Li, X., Otsuka, N., and Brigham, L. W.: Spatial and temporal variations of recent shipping along the Northern Sea Route, Polar Science, 27, 100 569, 2021.

Liu, Q., Babanin, A. V., Zieger, S., Young, I. R., and Guan, C.: Wind and wave climate in the Arctic Ocean as observed by altimeters, J.
495   Clim., 29, 7957–7975, 2016.

Maher, P. T.: Tourism futures in the Arctic, in: The Interconnected Arctic — UArctic Congress 2016, pp. 213–220, Springer, Cham, 2017.

Martínez-Alvarado, O., Baker, L. H., Gray, S. L., Methven, J., and Plant, R. S.: Distinguishing the cold conveyor belt and sting jet airstreams in an intense extra-tropical cyclone, Mon. Weather Rev., 142, 2571–2595, 2014.

Melia, N., Haines, K., and Hawkins, E.: Sea ice decline and 21st century trans-Arctic shipping routes, Geophys. Res. Lett.s, 43, 9720–9728,
500   2016.

National Snow & Ice Data Center: Sea Ice Index Animation Tool, pp. Accessed 11 Nov 2020, https://nsidc.org/data/seaice_index/archives/image_select, 2020.

Notz, D. and SIMIP Community: Arctic sea ice in CMIP6, Geophysical Research Letters, 47, e2019GL086 749, 2020.

Parkinson, C. L. and Comiso, J. C.: On the 2012 record low Arctic sea ice cover: Combined impact of preconditioning and an August storm,
505   Geophys. Res. Lett., 40, 1356–1361, 2013.

Peng, L., Zhang, X., Kim, J.-H., Cho, K.-H., Kim, B.-M., Wang, Z., and Tang, H.: Role of intense Arctic storm in accelerating summer sea ice melt: an in situ observational study, Geophys. Res. Lett., 48, e2021GL092 714, 2021.

Pinto, J. G., Karremann, M. K., Born, K., Della-Marta, P. M., and Klawa, M.: Loss potentials associated with European windstorms under future climate conditions, Climate Research, 54, 1–20, 2012.

510   Reed, R. J. and Kunkel, B. A.: The Arctic circulation in summer, J. Meteorol., 17, 489–506, 1960.

Schultz, D. M. and Browning, K. A.: What is a sting jet?, Weather, 72, 63–66, 2017.

Schultz, D. M., Keyser, D., and Bosart, L. F.: The effect of large-scale flow on low-level frontal structure and evolution in mid-latitude cyclones, Mon. Weather Rev., 126, 1767–1791, 1998.

Serreze, M. C., Lynch, A. H., and Clark, M. P.: The Arctic frontal zone as seen in the NCEP-NCAR reanalysis, J. Clim., 14, 1550–1567,
515   2001.

Shapiro, M. A. and Keyser, D.: Fronts, jet streams and the tropopause, in: Extratropical Cyclones: The Eric Palmen Memorial Volume, pp. 167–191, Springer, 1990.

Simmonds, I. and Keay, K.: Extraordinary September Arctic sea ice reductions and their relationships with storm behavior over 1979–2008, Geophys. Res. Lett., 36, 2009.

520 Simmonds, I. and Li, M.: Trends and variability in polar sea ice, global atmospheric circulations, and baroclinicity, Annals of the New York Academy of Sciences, 1504, 167–186, 2021.

Simmonds, I. and Rudeva, I.: The great Arctic cyclone of August 2012, Geophys. Res. Lett., 39, 2012.

Simmonds, I. and Rudeva, I.: A comparison of tracking methods for extreme cyclones in the Arctic basin, Tellus A: Dynamic Meteorology and Oceanography, 66, 25 252, 2014.

525 Simmonds, I., Burke, C., and Keay, K.: Arctic climate change as manifest in cyclone behavior, J. Clim., 21, 5777–5796, 2008.

Squire, V. A.: Ocean wave interactions with sea ice: A reappraisal, Annual Review of Fluid Mechanics, 52, 37–60, 2020.

Stroeve, J. C., Kattsov, V., Barrett, A., Serreze, M., Pavlova, T., Holland, M., and Meier, W. N.: Trends in Arctic sea ice extent from CMIP5, CMIP3 and observations, Geophys. Res. Lett., 39, 2012.

Tanaka, H. L., Yamagami, A., and Takahashi, S.: The structure and behavior of the Arctic cyclone in summer analyzed by the JRA-25/JCDAS
530 data, Polar Sci., 6, 55–69, 2012.

Tao, W., Zhang, J., and Zhang, X.: The role of stratosphere vortex downward intrusion in a long-lasting late-summer Arctic storm, Q. J. R. Meteorol. Soc., 143, 1953–1966, 2017.

Thomson, J. and Rogers, W. E.: Swell and sea in the emerging Arctic Ocean, Geophys. Res. Lett., 41, 3136–3140, 2014.

Varino, F., Arbogast, P., Joly, B., Riviere, G., Fandeur, M.-L., Bovy, H., and Granier, J.-B.: Northern Hemisphere extratropical winter cyclones
535 variability over the 20th century derived from ERA-20C reanalysis, Climate dynamics, 52, 1027–1048, 2019.

Vessey, A. F., Hodges, K. I., Shaffrey, L. C., and Day, J. J.: An inter-comparison of Arctic synoptic scale storms between four global reanalysis datasets, Clim. Dyn., 54, 2777–2795, 2020.

Wang, C.-C. and Rogers, J. C.: A composite study of explosive cyclogenesis in different sectors of the North Atlantic. Part I: Cyclone structure and evolution, Monthly Weather Review, 129, 1481–1499, 2001.

540 Waseda, T., Webb, A., Sato, K., Inoue, J., Kohout, A., Penrose, B., and Penrose, S.: Correlated increase of high ocean waves and winds in the ice-free waters of the Arctic Ocean, Sci. Rep., 8, https://doi.org/doi: 10.1038/s41598-018-22500-9, 2018.

Waseda, T., Nose, T., Kodaira, T., Sasmal, K., and Webb, A.: Climatic trends of extreme wave events caused by Arctic Cyclones in the western Arctic Ocean, Polar Science, 27, 100 625, 2021.

Wickström, S., Jonassen, M., Vihma, T., and Uotila, P.: Trends in cyclones in the high-latitude North Atlantic during 1979–2016, Quarterly
545 Journal of the Royal Meteorological Society, 146, 762–779, 2020.